Algal Neurotoxin Biosynthesis Repurposes the Terpene Cyclase Structural Fold Into an *N*-prenyltransferase

Jonathan R. Chekan[1], Shaun M. K. McKinnie[2], Joseph P. Noel[3], Bradley S. Moore[1,4]*

[1]Center for Marine Biotechnology and Biomedicine, Scripps Institution of Oceanography, University of California San Diego and [4]Skaggs School of Pharmacy and Pharmaceutical Sciences, University of California San Diego, La Jolla, CA, 92093, USA.

[2]Department of Chemistry and Biochemistry, University of California Santa Cruz, Santa Cruz, CA, 95064, USA.

[3]Jack H. Skirball Center for Chemical Biology and Proteomics, The Salk Institute for Biological Studies, La Jolla, California 92037, USA

Table of Contents

www.pnas.org/cgi/doi/10.1073/pnas.2001325117

Biological Methods

Cloning and Mutagenesis

PCR of genes was completed using PrimeStar HS DNA polymerase (Takara Bio), while the vector backbone was amplified using PrimeStar Max (Takara Bio). Protein expression constructions were generated in the pET28a vector using the NEBuilder HiFi DNA Assembly mix. Mutations were generated by a three-piece assembly using the vector, an N-terminal fragment containing the mutation, and a C-terminal fragment containing the mutation. Plasmids were purified from *Escherichia coli* DH5α cells and inserts were Sanger sequenced to confirm their identity. Vectors were transformed into *E. coli* BL-21 cells for subsequent expression. The DabA protein was constructed as Ser26 to C-term truncation to remove the N-terminal signal peptide. All subsequent DabA variants were based on this construct.

Protein Expression and Purification

E. coli BL-21 cells harboring the appropriate vector were grown overnight in 10 mL of lysogeny broth supplemented with 50 μg/mL kanamycin. A portion of the overnight culture (4 mL) was used to inoculate 1 L of terrific broth supplemented with 50 mg/L kanamycin in a 2.4 L Erlenmeyer flask. The flasks were placed in a 37 ^{o}C shaking incubator until the OD_{600} reached approximately 1. The incubator was then cooled to 18 ^{o}C, and the flasks were incubated for an additional 1 h. IPTG (0.5 mM final concentration) was added to induce protein expression, and the flasks were incubated for 18 h. Cells were harvested by centrifugation at 8,000 x g for 10 minutes and resuspended in buffer containing 500 mM NaCl, 20 mM Tris pH 8.0, and 10% glycerol. Cell pellets were frozen and stored at -70 ^{o}C.

Cells were lysed by sonication with a Qsonica 6 mm tip at 40% amplitude for 12 cycles of 15 seconds on and 45 seconds off. The lysate was centrifuged at 14,000 x g for 30 minutes to remove any insoluble debris. The supernatant was loaded onto a 5 mL HisTrap column (GE Healthcare) and washed with buffer A (1 M NaCl, 20 mM Tris pH 8.0, 30 mM imidazole). Protein was eluted using a linear gradient from 0-100% buffer B (1 M NaCl, 20 mM Tris pH 8.0, 250 mM imidazole) over 40 mL while collecting 5 mL fractions. Fractions were evaluated for purity by SDS-PAGE, and pure fractions were collected.

In the case of DabA used for crystallography, 100 U of thrombin were added to the pooled fractions immediately after purification by the HisTrap column, and the mixture was allowed to incubate for 18 h at 4 ^{o}C. Complete cleavage of the N-terminal His_6 tag was confirmed by SDS-PAGE. Protein was subsequently purified by size exclusion chromatography using a HiLoad 16/60 Superdex 75 prep grade column (GE Healthcare Life Sciences) pre-equilibrated with 100 mM KCl and 20 mM HEPES pH 7.5. Protein containing fractions were collected and concentrated with an Amicon Ultra-15 30 kDa centrifugal filter (Millipore Sigma) to approximately 15 mg/mL before aliquoting, freezing on dry ice, and storage at -70 ^{o}C.

If protein was not to be used for crystallography, pure fractions were directly taken after the HisTrap column and concentrated with an Amicon Ultra-15 30 kDa centrifugal filter (Millipore Sigma). The protein was further purified by size exclusion chromatography using a HiLoad 16/60 Superdex 75 prep grade column (GE Healthcare Life Sciences) pre-equilibrated with 300 mM NaCl, 10% glycerol, and 20 mM Tris pH 8.0. Protein containing fractions were collected and concentrated to approximately 15 mg/mL before aliquoting, freezing on dry ice, and storage at -70 ^{o}C.

Crystallography, Data Collection, Structure Determination, and Structure Refinement

DabA was screened using commercially available sparse matrix screens. Initial crystals were observed in the Wizard III screen (Rigaku Reagents), but could not be successfully optimized. Based on secondary

structure prediction and conservation, an N-terminal truncation was made creating a DabA Glu46 to C-term construct.

The activity of this construct was confirmed by an LC-MS activity assay using 5 mM L-Glu, 1 mM GPP, 5 mM $MgCl_2$, and 19 μM DabA variant in a reaction buffer containing 100 mM KCl, 20 mM HEPES pH 8.0, and 10% glycerol. The reaction was quenched after 2.5 h with 1 equiv. of 2% formic acid and analyzed using a Bruker amaZon Ion Trap and Agilent 1200 LC-MS with a Phenomenex Luna RP 5μ C18(2) 150 x 4.6 mm. The following method was used at flow rate of 0.75 mL/min: 5% B (1 min), 5 to 100% B (21 min), 100% B (1.5 min), 100 to 5% B (2.5 min), 5% B (2 min), wherein A = 0.1% aqueous formic acid, and B = 0.1% formic acid in acetonitrile.

The truncated protein was successfully optimized with hanging drop vapor diffusion as follows: 4 mg/mL protein was preincubated with 2 mM GSPP, 5 mM $MgCl_2$, and 50 mM L-Glu and mixed 1 μL : 1 μL with a mother liquor containing 1.5 M sodium citrate and 0.05 M HEPES pH 7.5. Crystals were grown over a well of 150 μL mother liquor and began to appear after one month at 9 °C. Crystals were transferred to fresh mother liquor supplemented with 2 mM GSPP, 5 mM $MgCl_2$, and 100 mM L-Glu for 24 h. Immediately prior to vitrification in LN_2, crystals were briefly soaked in mother liquor supplemented with 30% D-glucose, 2 mM GSPP, 5 mM $MgCl_2$, and 100 mM L-Glu. Manganese containing crystals were generated in a similar manner except $MgCl_2$ was replaced with $MnCl_2$ and a 3 h soak was used instead of a 24 h soak. For the NGG containing crystals, the mother liquor was composed of 1.35 M sodium citrate tribasic, 0.05 M HEPES pH 7.5, 5mM $MgCl_2$ and 2 mM NGG and DabA was used at a concentration of 8 mg/mL. NGG containing crystals were not soaked in fresh mother liquor and instead were briefly soaked in mother liquor supplemented with 30% D-glucose, 2 mM NGG, and 5 mM $MgCl_2$ prior to vitrification. All data were collected at the Advanced Light Source Macromolecular Crystallography beamline (8.2.1).

Diffraction data were indexed and scaled using autoPROC (1). Initial phases were determined by using a combination of SAD and molecular replacement. Specifically, crystals were soaked for 3 h in 1 mM methyl mercury chloride prior to vitrification. An initial DabA structure was generated from the weak anomalous signal found in the data set along with PDB code 5NX5 using MR-SAD in the Phenix software package (2). This low quality initial structure was used as the search model for PHASER (3) to obtain improved phases. A second model was built using a combination of Buccaneer (4) and Phenix autoBuild (2). The structure was improved by iterative manual adjustments in COOT (5) and refinement with REFMAC5 (6). All collection and refinement statistics are found in Table S2.

d_5-NGG and d_5-PKA Production

d_5-NGG and d_5-PKA were produced as internal standards to accurately normalize NGG and PKA enzymatic production between LC-MS runs. Both deuterium labeled compounds were produced enzymatically using either native DabA or KabA. A 300 μL solution containing 100 mM L-glutamic acid (2,3,3,4,4-d_5, 97-98%, Cambridge Isolate Laboratories), 1 mM DMAPP/GPP, 5 mM $MgCl_2$, 300 mM NaCl, 20 mM Tris pH 8.0, and 25 μM enzyme was incubated at 21 °C for 18 h. The reaction was filtered, diluted, aliquoted, and stored at -70 °C for later use.

Activity Assays

Activity assays were performed to test the effects of different mutations. Assays were completed in 50 μL total volume and contained 5 nM DabA variant, 5 mM $MgCl_2$, 25 mM L-glutamate pH 8.0, 100 μM GPP, 300 mM NaCl, and 20 mM Tris pH 8.0. Reactions were initiated with enzyme and, after 10 minutes, were quenched with 50 μL of 2% aqueous formic acid containing d_5-NGG. Samples were analyzed using a Bruker amaZon Ion Trap and Agilent 1200 LC-MS with a Synergi Polar-RP 4μ 250 x 4.6 mm column using the following method at a flow rate of 0.75 mL/min: 0% B (4.5 min), 0 to 5% B (0.5 min), 5 to 26% B (9 min), 26 to 80% B (9 min), 80 to

100% B (1 min), 100% B (1.5 min), 100 to 0% B (2.5 min), 0% B (2 min), wherein A = 0.1% aqueous formic acid, and B = 0.1% formic acid in acetonitrile. Extracted ion chromatograms for the expected NGG product mass, $[M-H]^{-1}$ = 282.2, were integrated. The peak areas were all normalized using the d_5-NGG present in the quenching solution. Each area was then normalized to the amount produced by WT DabA. Assays for each DabA variant were completed in triplicate.

Activity assays were completed to test the ability of DabA and KabA to utilize different prenyl donors. Assays were completed in 100 μL total volume and contained 2 μM DabA variant, 5 mM $MgCl_2$, 100 mM L-glutamate pH 8.0, 200 μM prenyl donor, 300 mM NaCl, and 20 mM Tris pH 8.0. Reactions were initiated with enzyme and, after 4.5 hours, were quenched with 100 μL of 2% aqueous formic acid. The majority of samples were analyzed for product formation by LC-MS using the method described for the mutagenesis assays. For the longer geranyl and farnesyl diphosphate substrate assays, the following method was used: 10% B (0.5 min), 10 to 100% B (19 min), 100% B (1.5 min), 100 to 10% B (2.5 min), 10% B (2 min), wherein A = 0.1% aqueous formic acid, and B = 0.1% formic acid in acetonitrile. The expected product mass was extracted for each assay.

Activity assays were completed to compare the ability of DabA to utilize different divalent cations as cofactors. Assays were completed in 50 μL total volume and contained 5 nM DabA, 5 mM of the chloride salt of the tested cation, 100 mM L-glutamate pH 8.0, 100 μM GPP, 300 mM NaCl, and 20 mM Tris pH 8.0. Reactions were initiated with enzyme and, after 10 minutes, were quenched with 50 μL of 2% aqueous formic acid containing d_5-NGG. Samples were analyzed for NGG production using the LC-MS procedure discussed in the kinetic assay protocol. Each run was integrated for NGG and d_5-NGG as described in the kinetic assay protocol and subsequently normalized to the d_5-NGG intensity. Assays were completed in quadruplicate and normalized to DabA catalyzed NGG production in the presence of $MgCl_2$.

Kinetic Assays

Individual assay conditions were optimized for each enzyme and substrate tested. In general, assays were completed on the 200 μL scale using 5-25 nM enzyme, 5 mM $MgCl_2$, 300 mM NaCl, and 20 mM Tris pH 8.0. For assays measuring kinetics of DMAPP or GPP, L-glutamate pH 8.0 was used at a constant concentration of 100 mM. For assays measuring kinetics of L-glutamate, DMAPP or GPP was used at a concentration of 100 μM. Reactions were initiated with the addition of enzyme and 50 μL was removed at 5, 10, and 15 minutes and quenched in 50 μL of 2% aqueous formic acid containing a standard amount of either d_5-NGG or d_5-PKA. Each reaction was analyzed using Agilent 1260 infinity HPLC and Bruker amaZon ion trap mass spectrometer LC-MS with a Phenomenex Luna 5μm $C_{18(2)}$ 100 Å 100 x 4.6 mm column using a 40 μL injection. For LC-MS analysis, Solvent A was water + 0.1% formic acid and Solvent B was acetonitrile + 0.1% formic acid and the flow rate was 0.75 mL/min.

The method to quantify NGG was: 20% Solvent B for 1.5 minutes; 20 to 100% Solvent B over 4.5 minutes; 100% Solvent B for 1 min; 100 to 20% Solvent B over 1 min; and 20% Solvent B for 3 min. Targeted MS/MS on $[M-H]^-$ of 282.2 *m/z* and 287.2 *m/z* with a width of 4 *m/z* was used to select for NGG and d_5-NGG respectively. The chromatogram for each run was extracted for the major MS^2 fragment (264.0 *m/z* and 267.8-269.2 *m/z* for NGG and d_5-NGG, respectively) and integrated. Peak areas were normalized to the deuterium labeled internal standard. A standard curve of NGG containing the d_5-NGG internal standard was generated and used to quantify NGG production over the course of the reaction.

The method to quantify PKA was 2% Solvent B for 1.5 minutes; 2 to 100% Solvent B over 4.5 minutes; 0% Solvent B for 1 min; 0 to 98% Solvent B over 1 min; and 2% Solvent B for 3 min. Targeted MS/MS on $[M-H]^-$ of 216.1 *m/z* and 221.1 *m/z* with a width of 4 *m/z* was used to select for PKA and d_5-PKA, respectively. The chromatogram for each run was extracted for the major MS^2 fragment (147.6 *m/z* and 152.6 *m/z* for PKA and d_5-PKA, respectively) and integrated. Peak areas were normalized to the deuterium labeled internal standard. A standard curve of PKA containing the d_5-PKA internal standard was generated and used to quantify PKA

production over the course of the reaction. All data points were completed in triplicate and data fit to the Michaelis-Menten equation using linear regression.

Phylogenetic Tree

Efforts to construct a focused phylogenetic tree to evaluate the evolutionary history of KabA and DabA were frustrated by the lack homologs on the amino acid level. Therefore, to construct a more global view of the placement of DabA/KabA within the terpene cyclase family, the entire InterPro families (7) for terpene cyclase-like 2 (IPR034686) and terpene cyclase-like 1, C-terminal domain (IPR034741) were chosen comprising a total of 9,125 sequences. To select representative members for tree construction, the sequences were clustered by amino acid sequence similarity with CD-HIT (8) using a cut off of 50% identity. A member from the 149 largest clusters was selected for inclusion in the tree. This process was repeated for the entire isoprenyl diphosphate synthase protein family (polyprenyl synthetase, PF00348), of which 50 representative sequences were included in the tree. In addition to these sequences, the closest DabA/KabA homologs as determined by BLASTp (TPR00180.1 and SCL16690.1) along with characterized red algal terpene cyclases (AXN72983.1, AZO92733.1, AZO92734.1, and ASV63464.1) were also added to the sequence list. Amino acid sequence alignments were completed with MAFFT (9) using the default parameters. A maximum likelihood tree was constructed with IQ-TREE (10) using the LG+F+R7 substitution model. This tree showed DabA/KabA separated from red algal terpene cyclases. To rigorously evaluate this observation, a constrained tree was created that forced the DabA/KabA proteins into the red algal branch. This tree was then evaluated using the approximately unbiased test (11) as implemented in IQ-TREE. A p-value of 0.000585 indicated that the constrained tree can be rejected and the DabA/KabA branch is phylogenetically distinct from red algal terpene cyclases.

Synthetic Methods

GPP (12), DMAPP (13), GSPP (14), and NGG (15) were chemically synthesized using established protocols and matched previous literature characterization.

Alternative organic pyrophosphate molecules were synthesized by adapting literature protocols (12). To a solution of tris (tetrabutylammonium) pyrophosphate (12) (0.5 g, 0.55 mmol) in dry acetonitrile (5 mL) at -35 °C was added alkenyl/alkynyl halide over 2 minutes. The reaction mixture was stirred at -35 °C for 10 minutes, then warmed to room temperature and stirred for 2 hours. The solvent was removed *in vacuo* and resuspended in minimal ion exchange buffer (25 mM NH_4HCO_3 in 2% aqueous isopropanol), then passed through 10 mL of DOWEX AG50W-X8 resin (NH_4 form), collecting the first 2 column volumes. The material was lyophilized, generating an off white solid, which was used without further purification.

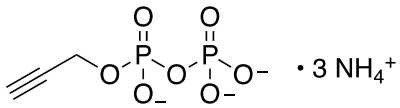

propargyl pyrophosphate trisammonium salt: ^{1}H-NMR (500 MHz, D_2O + 0.1% CH_3OH) δ 4.58 – 4.55 (m, 2H, -OC<u>H</u>$_2$), 2.88 (t, *J* = 2.4 Hz, 1H, CC-<u>H</u>); ^{13}C-NMR (125 MHz, D_2O + 0.1% CH_3OH) δ 80.3, 76.1, 54.2 (d, *J* = 4.0 Hz).

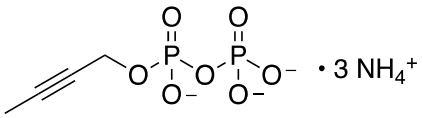

but-2-ynyl pyrophosphate trisammonium salt: ^{1}H-NMR (500 MHz, D_2O + 0.1% CH_3OH) δ 4.55 – 4.50 (m, 2H, -OC<u>H</u>$_2$), 1.85 – 1.84 (m, 3H, C≡C-<u>CH</u>$_3$); ^{13}C-NMR (125 MHz, D_2O + 0.1% CH_3OH) δ 85.0, 75.5, 55.3, 3.3.

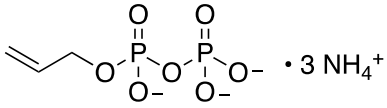

allyl pyrophosphate trisammonium salt: ^{1}H-NMR (500 MHz, D_2O + 0.1% CH_3OH) δ 6.00 (ddt, 1H, *J* = 17.9, 10.6, 7.4 Hz, -C<u>H</u>=CH$_2$), 5.38 (dd, 1H, *J* = 17.3, 1.8 Hz, -CH=C<u>H</u>$_2$), 5.25 – 5.19 (m, 1H, -CH=C<u>H</u>$_2$), 4.44 (dt, *J* = 7.5, 2.7 Hz, -OC<u>H</u>$_2$); ^{13}C-NMR (125 MHz, D_2O + 0.1% CH_3OH) δ 135.0, 117.5, 67.3 (d, *J* = 5.2 Hz).

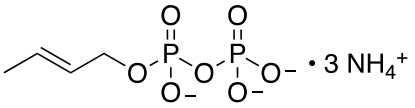

crotyl pyrophosphate trisammonium salt: ^{1}H-NMR (500 MHz, D_2O + 0.1% CH_3OH) δ 5.91 – 5.80 (m, 1H, C<u>H</u>=CHCH$_3$), 5.74 – 5.60 (m, 1H, -CH=C<u>H</u>CH$_3$), 4.43 – 4.33 (m, 2H, -OC<u>H</u>$_2$), 1.70 (d, *J* = 6.6 Hz, =CH<u>CH</u>$_3$); ^{13}C-NMR (125 MHz, D_2O + 0.1% CH_3OH) δ 131.7, 127.1, 67.5, 17.7.

Primer Name	Sequence
DabA S26 p28 NdeI F	GGTGCCGCGCGGCAGCCATATGATGTCGCACCCAAGCCAGCTCAATGCC
DabA E46 p28 NdeI F	GGTGCCGCGCGGCAGCCATATGGAAAGTCCGAAGGAAGTTCTCTCCCGC
DabA p28 HindIII Rev	GCTCGAGTGCGGCCGCAAGCTTTCAATTGAGGCGAACGGACTCAGACTCAACCGG
pET28 Up	CATATGGCTGCCGCGCGGCACC
pET28 Down	CT CGAGCACCACCACCACCACCACTGAG
DabA T119M For	ACAACCGGATTAACAGCGAGAAAATGTCAGCGATTTGCACC
DabA T119M Rev	GGTGCAAATCGCTGACATTTTCTCGCTGTTAATCCGGTTGT
DabA E335A For	GTGCACTAGCGATAGGGCAAGATTGGACGAAGATC
DabA E335A Rev	GATCTTCGTCCAATCTTGCCCTATCGCTAGTGCAC
DabA Y143F For	CGCATATTTTTACTCGATGATGTTCTATATCAATGATCAAACTGCTC
DabA Y143F Rev	GAGCAGTTTGATCATTGATATAGAACATCATCGAGTAAAAATATGCG
DabA R334A For	AACGATGTGTGCACTAGCGATGCGGAAAGATTGGACGAAG
DabA R334A Rev	CTTCGTCCAATCTTTCCGCATCGCTAGTGCACACATCGTT
DabA R423A For	GTGTCGAGGATGGGTACGCTGCTGACCACAAACC
DabA R423A Rev	GGTTTGTGGTCAGCAGCGTACCCATCCTCGACAC
DabA Y143A For:	TGTCGCATATTTTTACTCGATGATGGCCTATATCAATGATCAAACTGCTCAT
DabA Y143A Rev	ATGAGCAGTTTGATCATTGATATAGGCCATCATCGAGTAAAAATATGCGACA
DabA Y143L For	GTCGCATATTTTTACTCGATGATGTTATATATCAATGATCAAACTGCTCATC
DabA Y143L Rev	GATGAGCAGTTTGATCATTGATATATAACATCATCGAGTAAAAATATGCGAC
DabA H412A For	CTTTGATTGGGTATGTATTGGCCGAAGTTTGCTGTGTCGAGG
DabA H412A Rev	CCTCGACACAGCAAACTTCGGCCAATACATACCCAATCAAAG
DabA E413A For	TGGGTATGTATTGCACGCAGTTTGCTGTGTCGAGG
DabA E413A Rev	CCTCGACACAGCAAACTGCGTGCAATACATACCCA
KabA M114T For	ACAATCGTATAAATTGTGAGAAAACGGGTTCTTTGATGGCCC
KabA M114T Rev	GGGCCATCAAAGAACCCGTTTTCTCACAATTTATACGATTGT

Table S1. Primers for PCR

	DabA + Mg^{2+} + GSPP Complex	DabA + Mn^{2+} + GSPP Complex	DabA + Mg^{2+} + NGG Complex
Accession code	6VKZ	6VL0	6VL1
Data collection			
Space group	$P4_32_12$	$P4_32_12$	$P4_32_12$
Cell dimensions			
a, b, c (Å)	124.3, 124.3, 114.5	124.2, 124.2, 114.0	123.4, 123.4, 113.1
α, β, γ (°)	90.0, 90.0, 90.0	90.0, 90.0, 90.0	90.0, 90.0, 90.0
Resolution (Å)	42.1-2.10 (2.107-2.100)	50.0-2.20 (2.207-2.200)	49.6-2.10 (2.107-2.100)
R_{sym} (%)	13.0 (121.4)	13.2 (116.6)	12.3 (89.8)
R_{pim} (%)	3.9 (35.9)	4.6 (39.7)	2.9 (20.0)
$I / \sigma I$	16.6 (3.2)	15.8 (3.1)	22.7 (6.6)
Completeness (%)	94.9 (100)	90.9 (100)	100 (100)
Redundancy	11.8 (12.3)	9.4 (9.8)	19.0 (20.7)
$CC_{1/2}$	0.99 (0.78)	0.99 (0.81)	1.00 (0.96)
Refinement			
Resolution (Å)	42.1-2.1	41.0-2.2	42.0-2.1
No. reflections	50064	41668	51497
R_{work} / R_{free} (%)	16.6/18.8	17.8/20.3	17.7/19.5
No. atoms			
Protein	3581	3581	3578
Water	390	338	460
B-factors (Å^2)			
Protein	32.8	34.5	38.3
Water	42.2	42.2	46.5
Ligands	32.8	48.7	52.7
R.m.s. deviations			
Bond lengths (Å)	0.006	0.002	0.002
Bond angles (°)	0.771	0.415	0.477

1. Highest resolution shell is shown in parenthesis.
2. R-factor = $\Sigma(|F_{obs}|-k|F_{calc}|)/\Sigma |F_{obs}|$ and R-free is the R value for a test set of reflections consisting of a random 5% of the diffraction data not used in refinement.

Table S2. Refinement statistics for crystallography data.

Representative Terpene Cyclase Family Members Selected for Tree			
Q9X839	A0A010S4I9	A0A0A1Z8V8	A0A0B5IKE4
Q9K499	Q94G53	J7LH11	Q41594
A3KI17	B9S9Z3	B9RI00	B3TPQ6
A0A099D720	A0A287GX55	A8NE23	A0A0D3FK28
A0A069JMU8	Q6Q3H2	A0A066YQY7	A0A061F9B8
B2KSJ5	A0A0A8EZZ1	A0A072U8B8	A0A1S3YTU4
C7ASI9	A0A060SKA0	A0A076KZH5	A0A1C9J6A7
A0A097CSG2	Q82RR7	Q84LF0	A0A0L9V5C4
A0A097CS99	A0A071M9D1	A0A0J0BNS6	A0A072UZ75
B1W019	A0A0J8B437	O49853	Q84UU4
Q29VN2	A0A098DVT4	A0A072UXL6	A0A067JQ70
A0A014MUN6	B9RHP7	C5YHH7	A0A1S3Y8N1
A0A0D3FUB5	A0A1J6ID15	A0A0C1W9J4	A0A3S3NM43
O64961	A0A0L9TD46	A0A0D7CID6	P0DL13
A0A066U7L8	A0A0C5KR55	A0A0K8LQJ0	A0A0B2R155
B9RXW4	A0A0B2PNQ2	A4FVP2	A0A067D5M4
E2E2P0	A0A1E5W0J5	A0A067DG75	Q4KSH9
B9T825	A0A0D4DTS5	A0A0Q3I5V4	O48935
B0FGA9	A0A097ZQD8	A0A1L7U8F2	A0A0H5CEF0
A0A0C5L205	A0A072V8U9	A0A0C5KH39	A0A071M8M2
A0A067P991	A0A1B6PFB6	Q6PWU2	P0CJ43
D9XD61	A0A284QQE2	O24475	A0A022PQ06
A0A093V4V9	G1JUH1	B9SCB6	A0A0U1XXJ7
G5CV45	A0A059BXJ5	B9RPM3	P59287
Q9C6W6	A0A059C923	C7E5V7	Q5SBP3
I6QPS5	D2B747	B2J4A4	J7LQ09
A0A060SSS1	E3VWJ0	A0A0D3F4V0	I6RAQ6
E3W208	A0A0B2R0J5	H8ZM70	Q9C748
A0A077KIK5	A0A0F4JVJ9	A0A0I9YLV3	A0A287XU99
A0A077RZ53	A0A068UTJ4	A0A072TWP0	B6SCF5
A8NU13	O64404	A0A077KD00	A0A074RGB6
A0A084T0Z4	O81191	A0A077KMI1	E2E2N7
B9RXW0	D0VMR5	O65434	P0DPK6
A0A0Q3E1I9	B1B1U3	A0A061GGG2	A0A0J6XHN2
A0A0D3FIQ8	A0A014L5I1	A0A0D3FUB9	C7PLV2
B5HDJ6	A0A024RWJ3	Q9FXY7	A0A078FGP2
A0A0A9I9R9	A0A0B2PE61	B5A434	A0A0A7HJU3
Q8GUE4	A0A0B4L8B1	E4N7E5	

Isoprenoid Diterpene Synthases	
G0ADX0	A0A0Q7ST61
I6Z2B2	A0A1A5XT43
A0A1Q4YWQ4	M0M7F6
Q6D9C7	A0A0C4WT25
J3VTG0	A0A165J1L7
A0A0Q4X3R2	A0A1D1VRK9
A0A0G2J7S7	A0A096NR69
Q21C14	A0A1Y2GSF2
J3HXN3	L7LIX8
A0A089XEA0	A0A0A0EU98
D0CQB2	A0A0D2STX1
A0A1E5AGM0	B2HG97
A0A072MXL3	
A0A1Y0MHY3	
D7CG91	
A0A255YYE7	
D7MC20	
A0A1I6QVF3	
A0A0Q4FQ79	
A0A1C7D962	
A0A2G9HXL9	
X0RIU8	
A0A1I5EYD5	
A0A0U1KL63	
A0A061GKJ6	
A0A218Q5B7	
A0A098TKX4	
A0A1S3HNM6	
A0A1V3Q6R9	
A0A0F8D0C	
M3WGD6	
A0A1I6Y9A9	
G2R7P2	
A0A0Q4L888	
A0A1X7P3U6	
X5L2J3	
S2ZJN3	
A0A093V4V9	

Added Sequences
A0A505HLV2
A0A1C6RI17
A0A385AJM7
A0A3S9GV71
A0A3S9GVB5
A0A286R621

Table S3. List of UniProt accession codes for protein sequences used to construct the maximum likelihood phylogenetic tree. 199 were selected as representatives from the InterPro and 6 additional sequences were added as described on pg S5.

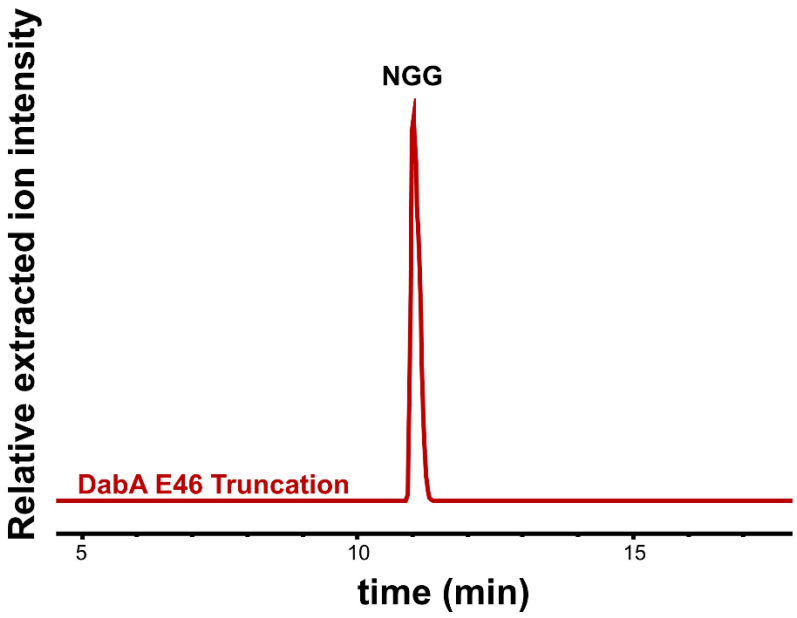

Figure S1: The DabA variant used for protein crystallography (DabA E46 to C-term) was tested to confirm it retained activity. The trace represents the EIC (extracted ion chromatogram) ± 0.5 *m/z* for the expected mass of the product, NGG (282.2 *m/z*).

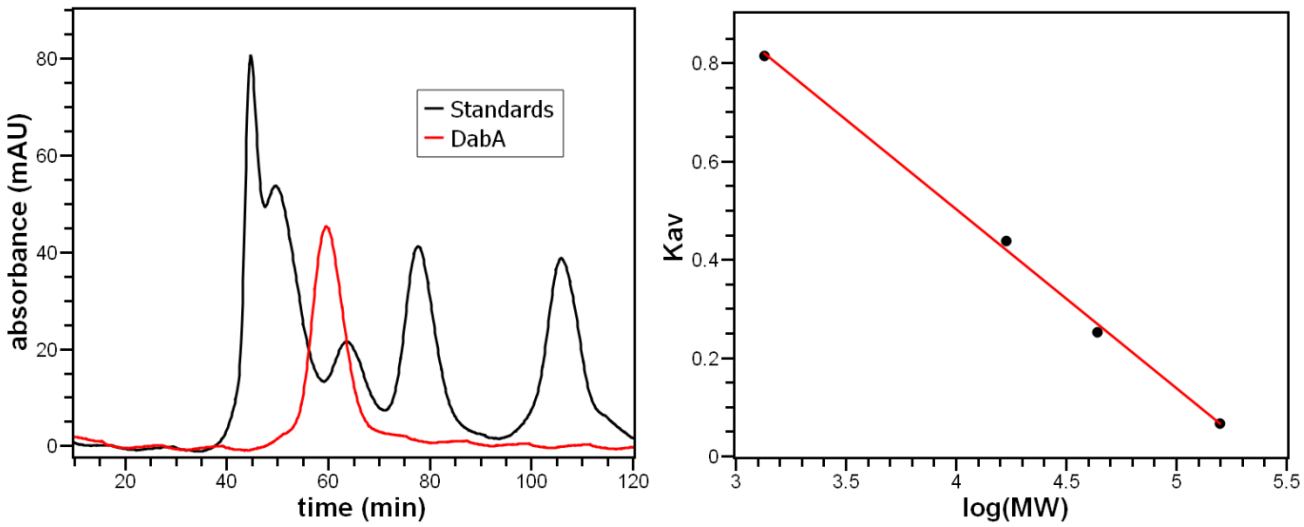

Figure S2: Gel filtration was used to estimate oligomerization state of DabA in solution. A standard curve was generated using BioRad Gel Filtration Standard (#1511901) and the experiment was completed on a HiLoad 16/60 Superdex 75 prep grade column. DabA eluted at 60 mins and was estimated to be 68.6 kDa. The molecular weight of the His_6-tag cut DabA Glu46 to C-term construct is 51.5 kDa. The calculated solution state is 1.3 monomers in size, and, therefore, DabA likely exists a monomer.

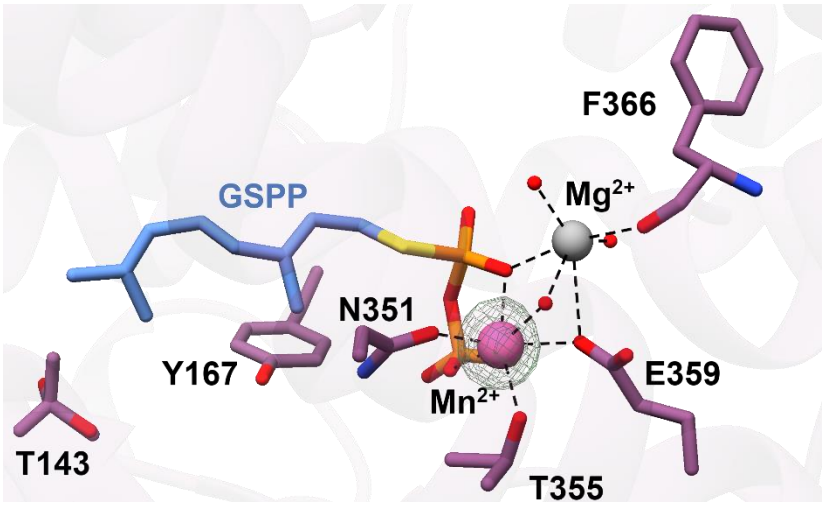

Figure S3: Active site of DabA in complex with GSPP. Crystals were soaked in a solution containing $MnCl_2$ in order to replace magnesium ions with the more electron dense manganese. F_o-F_c maps were generated by removing the manganese and completing refinement without the ion. Mesh was contoured to 10σ (green). Based on the observed electron density, manganese could successfully substitute for one of the two magnesiums.

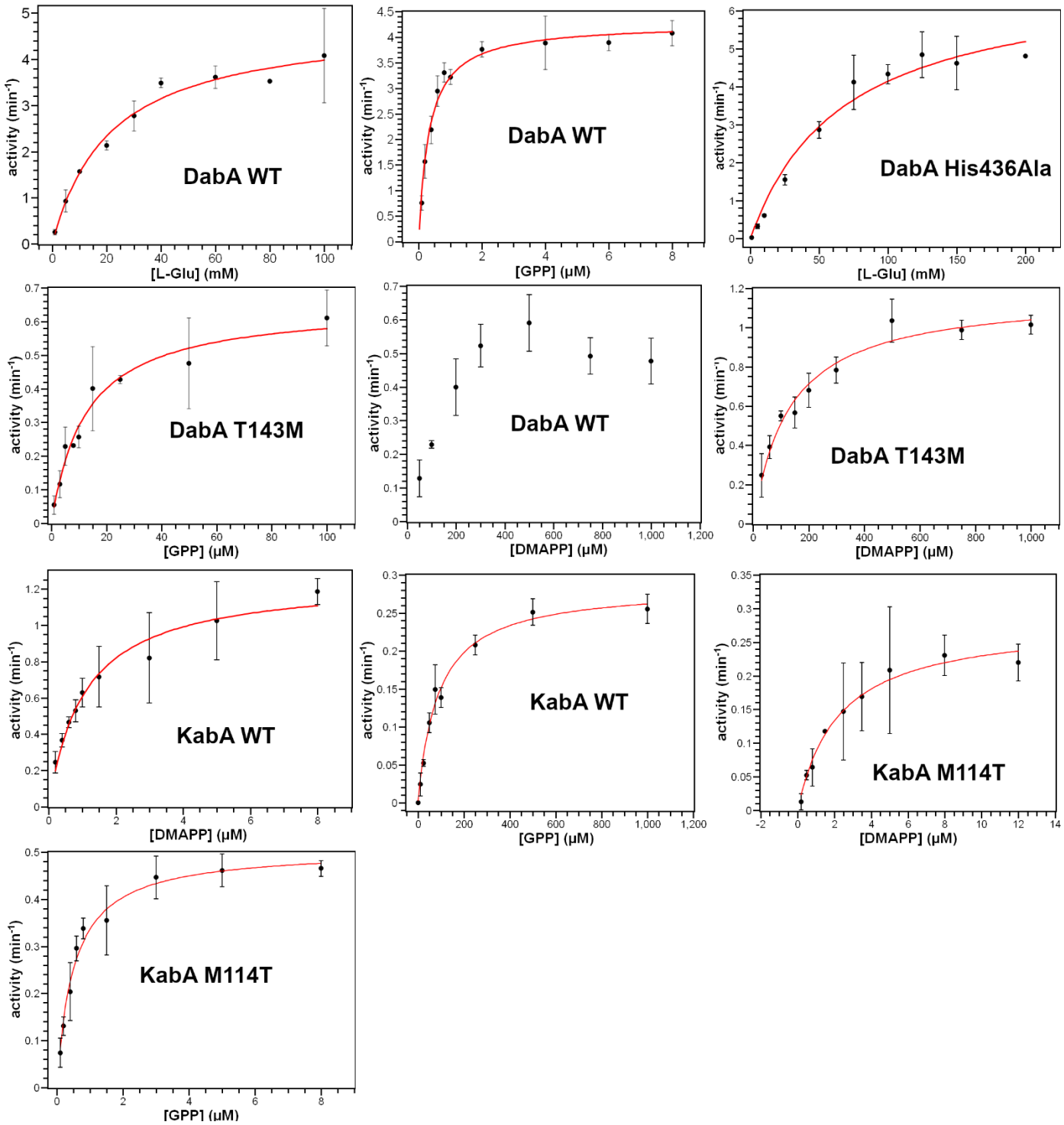

Figure S4. Kinetic analysis of DabA, KabA, and variants. Data was fit to the Michaelis-Menten equation. Each point was completed in triplicate. Values for kinetic parameters are found in Table 1. DabA did not display Michaelis-Menten kinetics when DMAPP was used as a substrate. This data was also fit to the substrate inhibition Michaelis-Menten equation, but the resulting constants were not physiologically relevant.

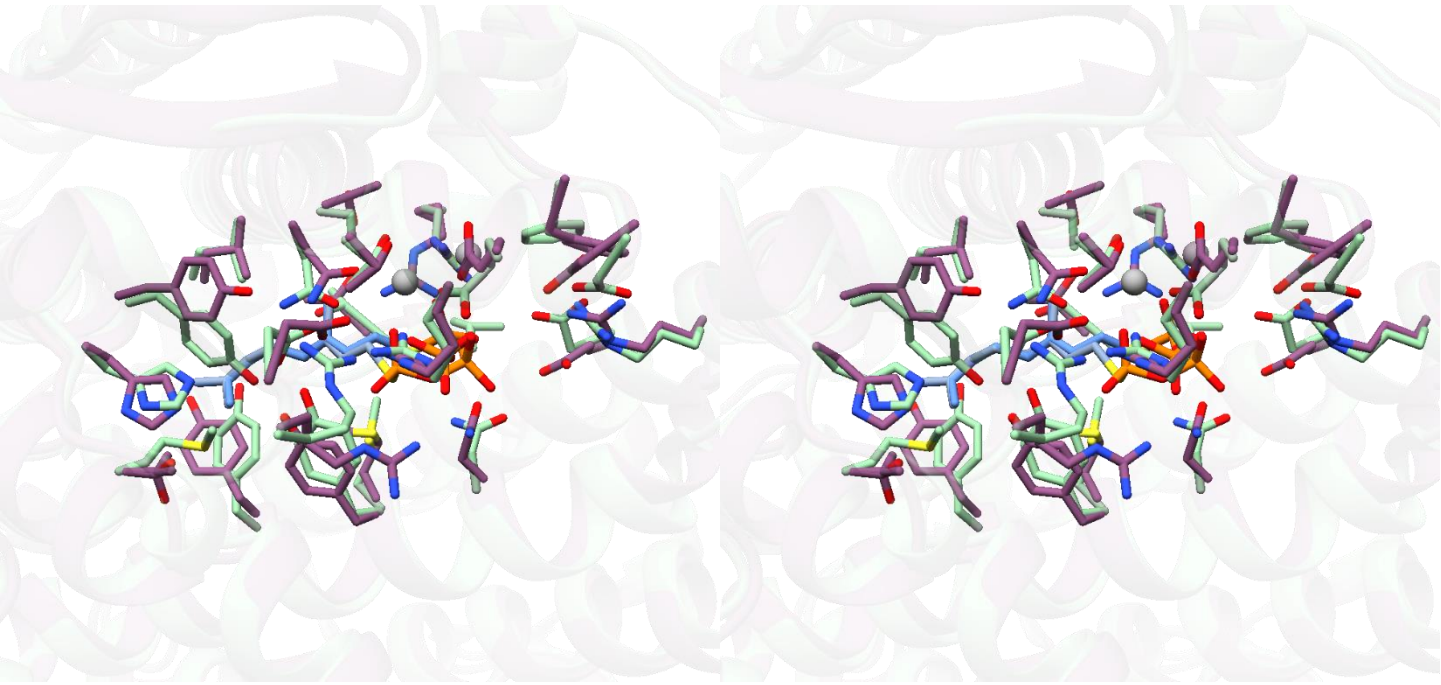

Figure S5: Stereoview of the DabA active site (purple) aligned with the KabA I-TASSER model (green). GSPP is shown in blue.

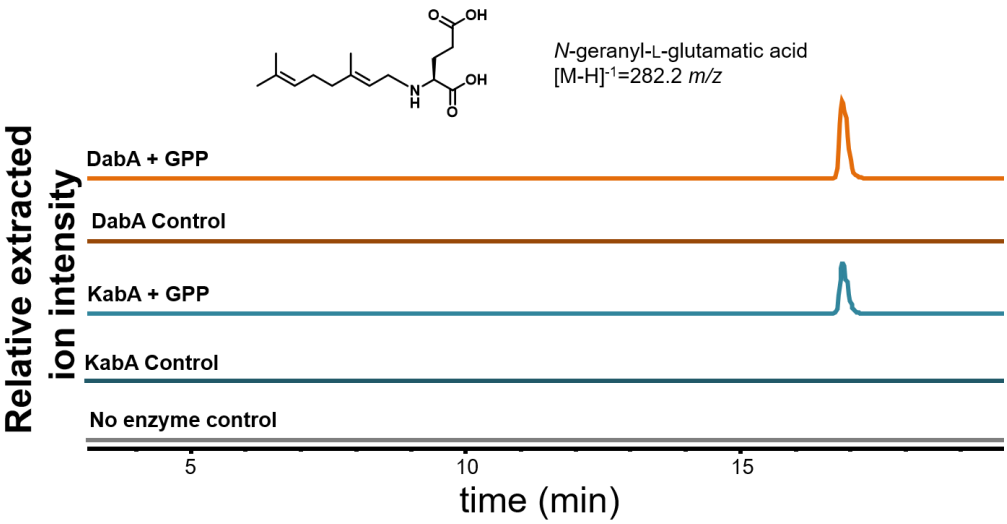
N-geranyl-L-glutamatic acid
[M-H]-1=282.2 m/z
Relative extracted ion intensity
DabA + GPP
DabA Control
KabA + GPP
KabA Control
No enzyme control
5
10
15
time (min)

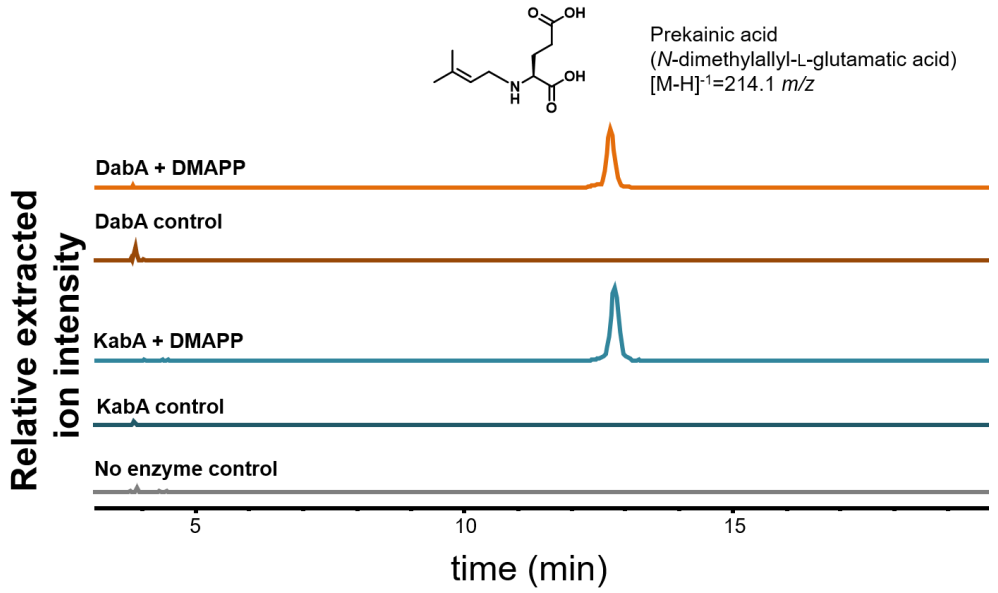
Prekainic acid
(N-dimethylallyl-L-glutamatic acid)
[M-H]-1=214.1 m/z
Relative extracted ion intensity
DabA + DMAPP
DabA control
KabA + DMAPP
KabA control
No enzyme control
5
10
15
time (min)

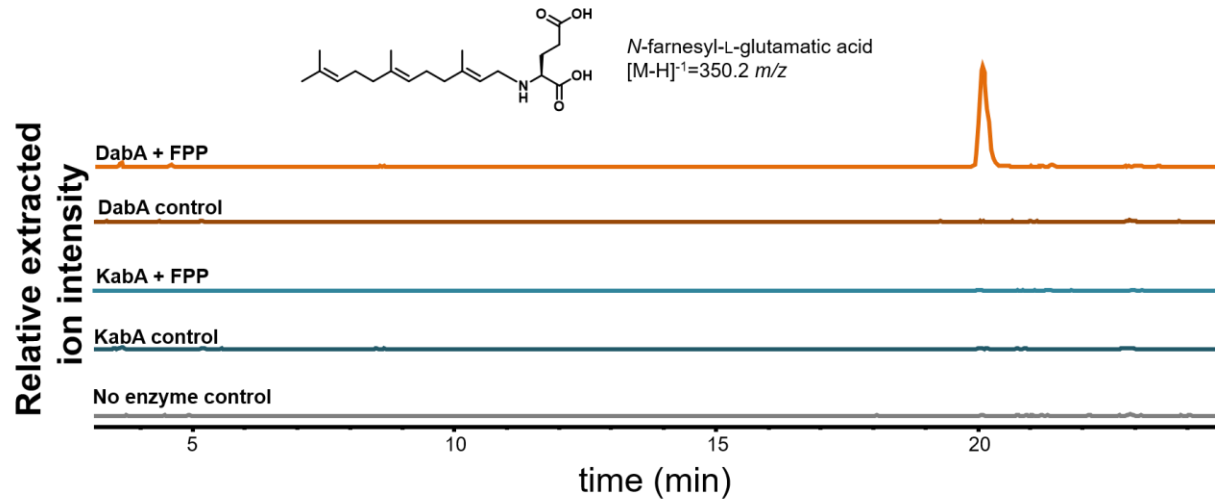
N-farnesyl-L-glutamatic acid
[M-H]-1=350.2 m/z
Relative extracted ion intensity
DabA + FPP
DabA control
KabA + FPP
KabA control
No enzyme control
5
10
15
20
time (min)

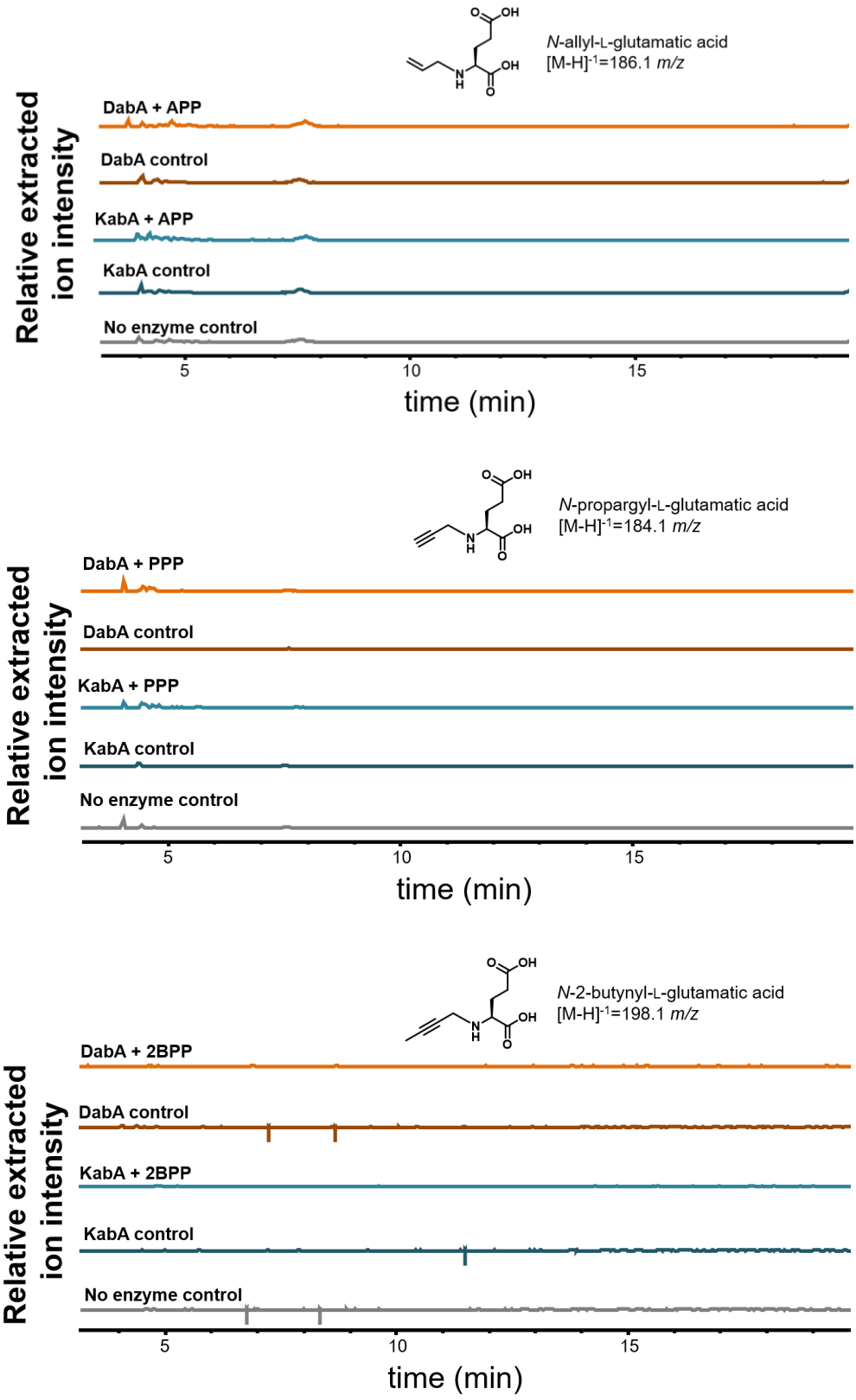
N-allyl-L-glutamatic acid
[M-H]-1=186.1 m/z
DabA + APP
DabA control
KabA + APP
KabA control
No enzyme control
Relative extracted ion intensity
5
10
15
time (min)
N-propargyl-L-glutamatic acid
[M-H]-1=184.1 m/z
DabA + PPP
DabA control
KabA + PPP
KabA control
No enzyme control
Relative extracted ion intensity
5
10
15
time (min)
N-2-butynyl-L-glutamatic acid
[M-H]-1=198.1 m/z
DabA + 2BPP
DabA control
KabA + 2BPP
KabA control
No enzyme control
Relative extracted ion intensity
5
10
15
time (min)

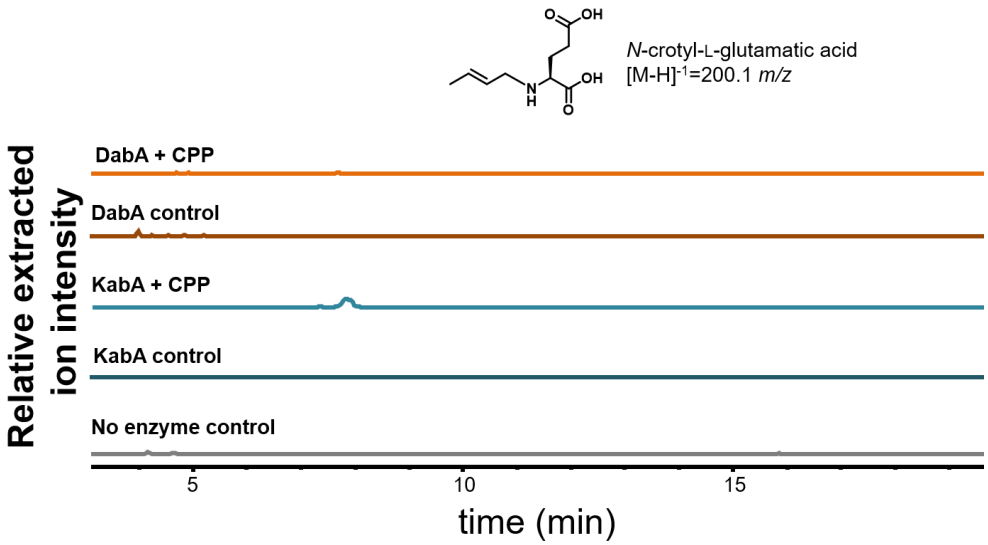

Figure S6: Both KabA and DabA were tested with a variety of organic diphosphates to evaluate their substrate specificity. Each trace is the EIC (extracted ion chromatogram) ± 0.5 *m/z* for the expected mass of the product indicated. The “DabA and KabA controls” lacked the prenyl diphosphate while the “No enzyme control” lacked enzyme. Substrate abbreviations are as follows: GPP (geranyl diphosphate), DMAPP (dimethylallyl diphosphate), FPP (farnesyl diphosphate), PPP (propargyl diphosphate), 2BPP (2-butynyl diphosphate), APP (allyl diphosphate), and CPP (crotyl diphosphate).

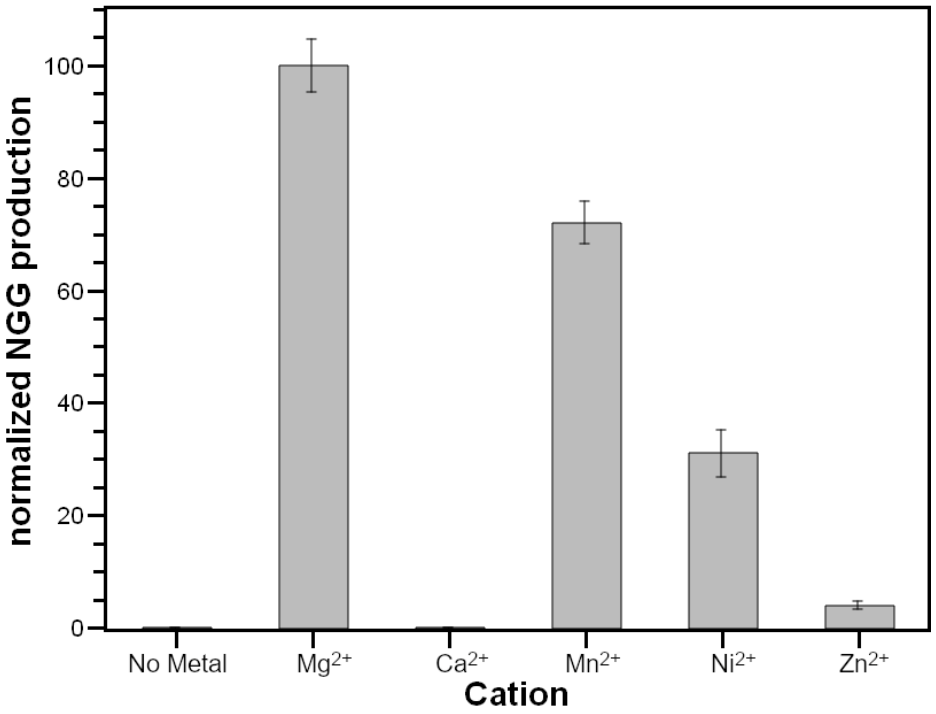

Figure S7: DabA activity assays were completed with either $MgCl_2$, $CaCl_2$, $MnCl_2$, $NiCl_2$, $ZnCl_2$, or no added metal to evaluate the importance of the identity of the cation for catalysis. While several metals can be used for catalysis, magnesium appears to be the favored divalent cation.

Supplementary References

1. Vonrhein C, et al. (2011) Data processing and analysis with the autoPROC toolbox. *Acta Crystallogr Sect D Biol Crystallogr* 67(4):293–302.
2. Adams PD, et al. (2010) PHENIX: A comprehensive Python-based system for macromolecular structure solution. *Acta Crystallogr Sect D Biol Crystallogr* 66(2):213–221.
3. McCoy AJ, et al. (2007) Phaser crystallographic software. *J Appl Crystallogr* 40(4):658–674.
4. Cowtan K (2006) The Buccaneer software for automated model building. 1. Tracing protein chains. *Acta Crystallogr Sect D Biol Crystallogr* 62(9):1002–1011.
5. Emsley P, Lohkamp B, Scott WG, Cowtan K (2010) Features and development of Coot. *Acta Crystallogr D Biol Crystallogr* 66(Pt 4):486–501.
6. Vagin AA, et al. (2004) REFMAC5 dictionary: Organization of prior chemical knowledge and guidelines for its use. *Acta Crystallogr Sect D Biol Crystallogr* 60(12 I):2184–2195.
7. Mitchell AL, et al. (2019) InterPro in 2019: Improving coverage, classification and access to protein sequence annotations. *Nucleic Acids Res* 47(D1):D351–D360.
8. Huang Y, Niu B, Gao Y, Fu L, Li W (2010) CD-HIT Suite: A web server for clustering and comparing biological sequences. *Bioinformatics* 26(5):680–682.
9. Katoh K, Rozewicki J, Yamada KD (2017) MAFFT online service: multiple sequence alignment, interactive sequence choice and visualization. *Brief Bioinform* (June):1–7.
10. Nguyen LT, Schmidt HA, Von Haeseler A, Minh BQ (2015) IQ-TREE: A fast and effective stochastic algorithm for estimating maximum-likelihood phylogenies. *Mol Biol Evol* 32(1):268–274.
11. Shimodaira H (2002) An approximately unbiased test of phylogenetic tree selection. *Syst Biol* 51(3):492–508.
12. Woodside AB, Huang Z, Poulter CD (1988) Trisammonium geranyl diphosphate. *Org Synth* 66:211–216.
13. Chekan JR, et al. (2019) Scalable biosynthesis of the seaweed neurochemical, kainic acid. *Angew Chemie Int Ed* 58(25):8454–8457.
14. Phan RM, Poulter CD (2000) Synthesis of geranyl *S*-thiolodiphosphate. A new alternative substrate/inhibitor for prenyltransferases. *Org Lett* 2(15):2287–2289.
15. Brunson JK, et al. (2018) Biosynthesis of the neurotoxin domoic acid in a bloom-forming diatom. *Science* 361(6409):1356–1358.